RSC Advances

ROYAL SOCIETY OF CHEMISTRY

www.rsc.org/advances

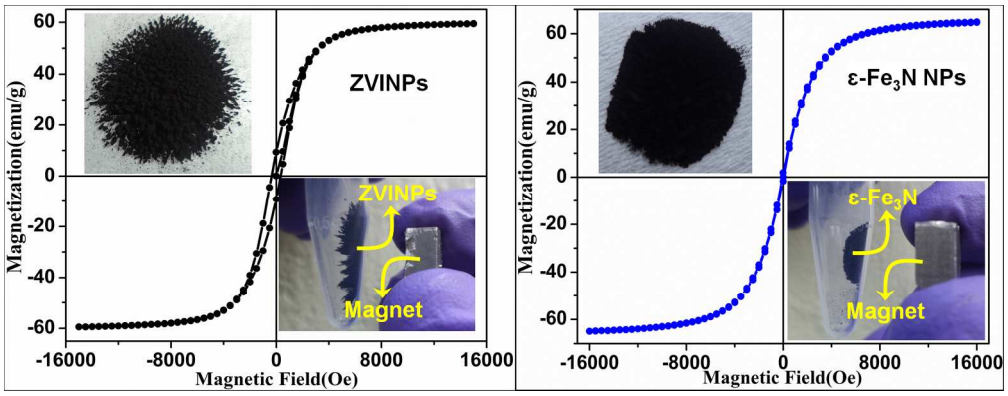

We have demonstrated the large-scale synthesis of highly magnetic and stable iron nitride nanoparticles through nitridation of zero-valent iron nanoparticles
374x144mm (150 x 150 DPI)

Journal Name

COMMUNICATION

Large scale synthesis and formation mechanism of highly magnetic and stable iron nitride (ε-Fe_3N) nanoparticles

Received 00th January 20xx,
Accepted 00th January 20xx

DOI: 10.1039/x0xx00000x

www.rsc.org/

Rohith Vinod K.,[a] P. Saravanan,[b] M. Sakar,[a] V. T. P. Vinod,[c] Miroslav Cernik[c] and S. Balakumar,[a,*]

ε-Fe_3N magnetic nanoparticles with average size of 45 nm were synthesized by nitriding the zero valent iron nanoparticle precursors using ammonia gas as a reactive ambience. The technique reported in this study is found to be promising in producing highly stable ε-Fe_3N magnetic nanoparticles and can be extended to other forms of Fe-nitrides.

Nitrides of different transition metals have gained technological importance owing to their enhanced magnetic properties coupled with greater stability and corrosion resistance.[1,2] It is found that the physical and chemical properties of these materials are essentially depending upon the nitrogen content in the system.[3] Iron nitrides, as a subject of research revealed that the nitrogen content is dependent on the diverse crystal structures and phases of iron nitrides, such as γ-FeN (NaCl structure), ξ-Fe_2N (orthorhombic structure), ε-$Fe_{3-2}N$ (hexagonal structure), γ'-Fe_4N and α''-$Fe_{16}N_2$ (cubic structure).[4] The manipulation of nitrogen content in the iron nitrides allows to tune the magnetic properties to a larger extent. For instance, α''-$Fe_{16}N_2$ phases possess enhanced hard magnetic properties that can replace the existing rare-earth permanent magnets.[5] Among the various synthesis strategies of iron nitride phases, the nitridation process is one of renowned techniques, which has greater ability in producing materials with required magnetic phases and high stability.[6] However, the process of nitridation entails a customized environment, wherein a nitrogen-rich atmosphere is needed for the incorporation of nitrogen into Fe-lattices. Besides, this process also demands a highly reducing atmosphere to avoid possible oxidation. Under such circumstances, it becomes more difficult to control the size of particles especially at nanoscale. The methods, which addresses the above issues are often found to be chemical deposition techniques.[7] Alternatively, we herein report a facile nitridation process to form the iron nitride phase through nitriding the freshly prepared zero-valent iron nanoparticles (ZVINPs), in the ammonia ambience under an optimized nitridation temperature.

The chemical regents used in the experiments were of high purity (99.99%), procured from Sigma Aldrich. Initially, the ZVINPs were synthesized by chemical reduction method. In a typical procedure, an equivalent gram of 0.04 M $FeCl_2$ is homogeneously dissolved in 30 ml ethanol. To this, a 100 ml of 0.1 M sodium borohydride ($NaBH_4$) solution is added to precipitate the product that appeared to be black in colour, indicated the formation of ZVINPs (Fe^0). Further, this precipitation was washed several times with ethanol and dried in vacuum at 120 ^{0}C for 1 h. To prepare the iron nitride NPs, a required amount of freshly prepared ZVINPs is taken in an alumina boat and loaded into a tubular furnace where the ammonia (NH_3) gas is purged in the background at a flow rate of 100 mL/min. Then, the temperature of the furnace is raised to 650 ^{0}C and kept for 4 h to perform the nitridation process.

Both crystal structure and phase formation of the synthesized ZVINPs and ε-Fe_3N NPs (FNNPs) were analysed using powder X-ray diffraction (XRD) technique and the obtained results are showed in Figs. 1(a) and(b), respectively.

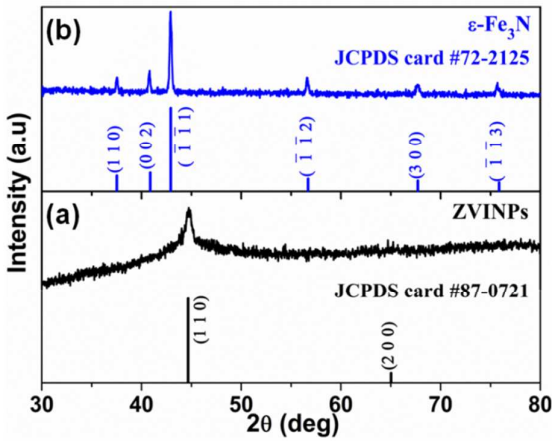

Fig. 1. XRD pattern of **(a)** Zero-valent iron NPs (Fe^0 NPs) and **(b)** ε-Fe_3N NPs.

[a] *National Centre for Nanoscience and Nanotechnology, University of Madras, Guindy campus, Chennai 600 025, India. Fax: 044-22352494/22353309; Tel: 044-22202749; *E-mail: balasuga@yahoo.com*
[b] *Defence Metallurgical Research Laboratory, Hyderabad 500 058, India.*
[c] *Institute for Nanomaterials, Advanced Technology and Innovation, Department of Natural Sciences, Technical University of Liberec, Studentská 1402/2, 46117 Liberec, Czech Republic.*

The XRD patterns are found to be consistent with the JCPDS card # 87-0721 and # 72-2125 that corresponds to the body-centered cubic structure with $Im\bar{3}m$ (229) space group of Fe^0 (ZVINPs) and hexagonal structure with $P312$(149) space group of ε-Fe_3N phases respectively. The average crystallite size of the ZVINPs and FNNPs was calculated from the Scherrer's formula (t = 0.94 λ/β cosΘ) and found to be 11 and 16 nm, respectively. It should be noted that no additional peaks corresponding to any other phase is observed in the XRD patterns. This indicates that the synthesized ZVINPs and FNNPs are stable and resistive to the formation of oxides. In addition to the structural analysis, the compositional analysis of the synthesized iron nitride nanoparticles was also carried out using the energy dispersive X-ray (EDX) spectroscopy analysis towards ascertaining the compositional confirmation of ε-Fe_3N phase. The results of EDX analysis are provided in the electronic supplementary information (ESI) file.

The formation mechanism of FNNPs involves simultaneous surface reduction and diffusion processes under an adequate reactive gas ambience and temperature.[8] In the nitridation process, the optimized temperature of 650 ^{0}C dissociates the NH_3 gas into hydrogen and nitrogen species, according to the equation: $2NH_3 \rightarrow 3H_2 + 2N$. Subsequently, the hydrogen species reduces the surface of ZVINPs and the nitrogen species diffuse into the lattice of Fe that leads to the formation of FNNPs. The schematic representation of FNNPs formation and the photographic images of the synthesized ZVINPs and FNNPs are shown in Figs. 2(a)-(c). In a typical experiment, iron chloride precursor was taken around 0.47 g and the chemical reduction process yielded around 0.21 g of ZVINPs (Fig. 2(b)), while the nitridation of ZVINPs yielded around 0.23 g of FNNPs (Fig. 2(c)). Such enhanced yields obtained in a single-shot process provide a possible scope for the large-scale synthesis of FNNPs in a cost effective approach.

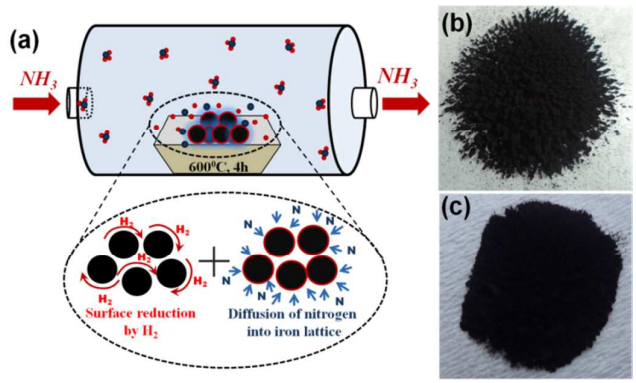

Fig. 2 Schematic representation of (a) nitridation process and formation mechanism of ε-Fe_3N NPs, and the photographic images of the synthesized powders of (b) Fe^0 ~ 0.21 g, (c) ε-Fe_3N NPs ~ 0.23 g.

In another experiment, the nitridation process was not occurred when the nitrogen ambience (at a flow rate of 100 mL/min) was employed (results are not shown here), indicating that the role of surface reduction by hydrogen species is found to be crucial as it modifies the surface of ZVINPs and makes the nitrogen diffusion effective and easier.[9] Such observations suggest that the formation of various nitride phases could be possible by controlling concentration of NH_3 gas (flow rate) and nitridation temperature with controlled heating rate and soaking period.

The size and morphology of the synthesized ZVINPs and FNNPs were analyzed using field emission scanning electron microscopy (FESEM) and the representative images obtained are shown in Figs. 3(a)-(d) and a few more images are provided in Fig. S2(a)-(d) as a supporting information (ESI). The morphology of the particles is found to be spherical for both the ZVINPs, as well as FNNPs and their average particle size is found to be 32 nm and 45 nm, respectively. The observed increment in the particle size of FNNPs compared to ZVINPs could be explained as follows. It should be noted that the formation of nanoscale iron nitride particles is essentially mediated by the ZVINPs, which is used as a precursor for FNNPs. Therefore, any changes in the particle size could be ascribed to the modifications occurred in ZVINPs during the nitridation process. Accordingly, in the course of nitridation process, there are essentially two factors which could influence the particle size of FNNPs: (i) the diffusion of N atoms into the lattices of Fe, which leads to the lattice expansion and (ii) the influence of nitridation temperature on the grain-size of particles. Considering, the concept of lattice expansion, it is possible for such microscopic changes occurred in Fe system, due to the diffusion of N atoms, could cause the macroscopic changes in the system, which is the increment in the particle sizes. Similarly, it is known that at the elevated temperatures, it is hardly possible to control the grain-size of the nanoparticles as the temperature becomes most influential factor on the particle growth due to the thermo-dynamical properties of nanoparticles.

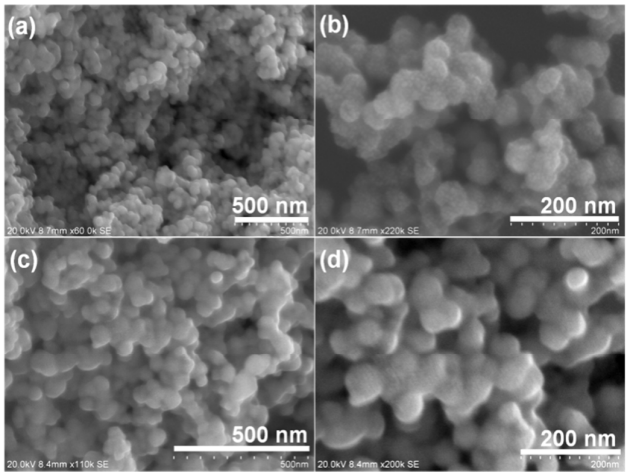

Fig. 3 FESEM micrographs of (a) and (b) zero-valent iron NPs; showing the spherical morphology with average size of 30 nm and (c) and (d) ε-Fe_3N NPs; showing spherical morphology with average particle size of 45 nm.

However, the nitridation process did not largely influence the particle size, morphology and their distributions, which could be attributed to the stability of the host ZVINPs. This suggests that the current strategy of nitriding the ZVINPs is a

straight forward method to produce highly stable nanoscale iron nitride phases.

The room temperature field-dependent magnetization (*M-H* hysteresis) properties of synthesized ZVINPs and FNNPs analyzed using the super conducting quantum interference device (SQUID) magnetometer at a maximum applied field of 16 kOe are shown in Figs. 4(a) and (b), respectively. The inset images of Fig. 4(a)-(b) placed at the bottom-right corner show the magnetically attractive nature of ZVINPs and FNNPs respectively, where they demonstrate excellent magnetic attraction even when the magnet is kept at a distance from the samples.

It is evident from the *M-H* curves that both the systems possess the room temperature ferromagnetic (FM) properties. The magnetic parameters such as the coercive field (H_c), saturation magnetization (M_s) and remanent magnetization (M_r) are found to be 335 Oe, 59.5 and 9.3 emu/g respectively for ZVINPs, and 65 Oe, 65.1 and 1.9 emu/g respectively for FNNPs.

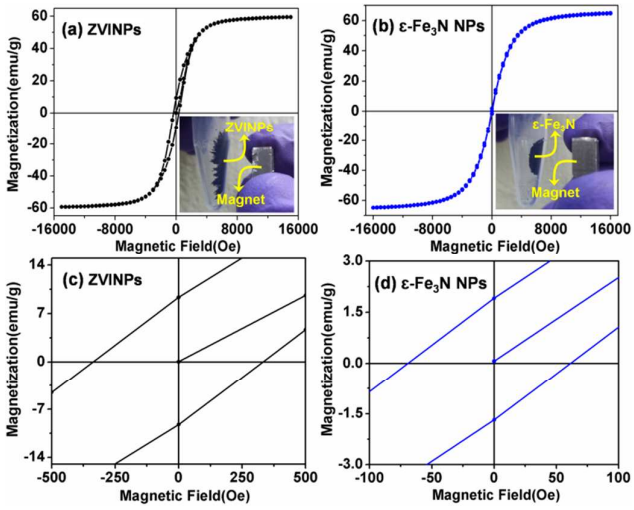

Fig. 4 Room temperature *M-H* hysteresis curve of (a) zero-valent iron NPs (Inset: Powders of ZVINPs), (b) ε-Fe_3N NPs (Inset: Powders of *ε*-Fe_3N NPs) (c) close image of *M-H* ZVINPs and (d) close image of *M-H* ZVINPs.

However, a noticeable difference is observed in the *M-H* curves where the hysteresis trend of FNNPs is appeared to be superparamagnetic (SPM). It should be noted that the SPM is the size effect of ferromagnetism. Alternatively, the SPM behaviour may also be manifested by the materials that possess an imbalanced distribution of up-spin states and down-spin states of the electrons in the system with easy axis of magnetization.[10] In ε-Fe_3N, the characteristic interactions between the electronic spins of Fe-lattice and N atoms causes the net magnetic moments in the system. Considering the crystal structure, ε-Fe_3N is a hexagonal system where the nitrogen atoms occupy only one-third (1/3) of the octahedral interstitials.[11] In such configuration, the spin of the electrons in nitrogen would be largely influenced. This in turn shields the 4*s* electrons of Fe and enhances the interactions of Fe 3*d*-N 2p electrons, which establishes a covalent bond between Fe and N atoms.[12-14] Therefore, the number of unpaired '*d*' electrons available for the magnetization in Fe is reduced and leads to the alteration in the magnitude of the net magnetic moments in the FNNPs compared to ZVINPs that switches the system from ferromagnetic to superparamagnetic. Further, this SPM behaviour could also be substantiated from the observed smaller coercive field for the FNNPs, as compared to the ZVINPs (Figs. 4c and d).

The temperature dependent magnetization (*M-T*) of Fe^0 and ε-Fe_3N nanoparticles in a constant applied field of 100 Oe is clearly manifested using the zero field cooled and field cooled (ZFC-FC) curves in Figs. 5(a) and (b) respectively.

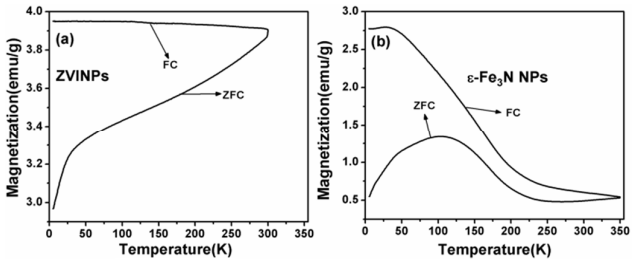

Fig. 5 Temperature dependent magnetic *M-T* curve (ZFC-FC profiles) of **(a)** zero-valent iron NPs and **(b)** ε-Fe_3N NPs.

In the *M-T* curve of ZVINPs, it can be observed a rapid increase in the magnetization below 30 K during the ZFC measurement and a gradual increase in the magnetization above 30 K. On the other hand, only a slight increase can be noticed in the magnetization in the FC measurement. The initial magnetization of 2.97 emu/g during ZFC could be induced by the small applied field due to the high ferromagnetic nature of Fe^0 nanoparticles. An abrupt enhancement in the magnetization bellow 30 K is due to the unblocking of Fe magnetic moments presumably located at surface of ZVINPs. As the surface phenomena is considerably large in the case of nanoparticles, the unblocking of the total surface magnetic moments result in a rapid augmentation in net magnetization. As the temperature increases, all the moments get released and dipoles get aligned in the direction of applied field, which gives a gradual raise in the net magnetization up to 300 K. The slight increase in the FC curve is the result of unsaturated condition. Absence of a specific blocking temperature (T_B) could be due to the insufficient temperature or applied field for the total magnetization of the entire magnetic moments in ZVINPs.[15] Further, the absence of any overlapping between ZFC and FC curves in the entire temperature range of 5 to 300 K is due to fact that the ZVINPs does not completely reached the superparamagnetic regime.[16]

In the case of ε-Fe_3N nanoparticles, the observed rapid increase in magnetization up to 1.34 emu/g with increasing temperature up to 110 K could be due to the blocked state of the magnetic moments that indicates the emergence of the superparamagnetic properties in the system. Further increase in temperature causes a gradual decrease in the magnetization due to the release of blocked state of magnetic moments in the random directions.

The ZFC-FC profile of ε-Fe_3N NPs can be understood in the basis of alignment of magnetic dipoles in the system with respect to the variation in temperature in the presence of a small applied field (100 Oe).[17] Initially, the system is frozen down to 5 K in absence of field, where the vector sum of randomly aligned magnetic dipoles in the ferromagnetic system has its minimum value. When a small magnetic field $H<H_K$ (H_K is the uniaxial anisotropic field) is applied, the magnetic dipole of domains aligned along the easy axis which is parallel or anti-parallel directions to the applied field with an energy difference of $E_b = K_uV$ (where K_u is the uniaxial anisotropic constant and V is the particle volume).[18] However, the net magnetization is the vector sum of magnetization of each magnetic dipole and hence, when temperature increases magnetization also increases and at a temperature above T_B the magnetic dipoles of the domains abruptly switches between parallel and anti-parallel directions due to the low field-high temperature limit of the system and thereby the net magnetization is deteriorated in the system. In the FC measurements, the magnetization of the system increases with decreasing temperature and at sufficiently lower temperature, the magnetic moment reaches the stable state. Further, the observed thermo-irreversibility in the ZFC-FC curves indicates the existence of ferromagnetic-superparamagnetic properties of the system that could be originated due to the inhomogeneous magnetic domains of the nanoparticles.[19, 20]

In conclusion, a facile nitridation process for the synthesis of nanosized ε-Fe_3N particles is demonstrated. Zero-valent iron nanoparticles (ZVINPs) were used as precursor material for the synthesis of iron nitride nanoparticles (FNNPs), where the ammonia gas was used as the reactive ambience. The nitridation process essentially involves the surface reduction of ZVINPs by hydrogen and subsequent diffusion of nitrogen into the Fe-lattice. The XRD results confirmed the formation of Fe and ε-Fe_3N phases in the ZVINPs and FNNPs, respectively. With the FESEM analysis, the morphology of the particles is found to be spherical and average particle size of ZVINPs and FNNPs is measured to be 32 and 45 nm, respectively. The magnetization studies by SQUID magnetometer revealed the ferromagnetic and superparamagnetic (SPM) behaviour for the ZVINPs and FNNPs, respectively. The manifestation of SPM characteristics in the FNNPs could be due to the interaction between the magnetic spins of Fe 3*d*-N 2*p* electrons in the system. The results of present study suggest that the current strategy of nitridation process would provide possible scope for large-scale synthesis of stable and highly magnetic FNNPs.

Acknowledgements

Authors gratefully acknowledge the Defence Research and Development Organization (DRDO), and one of the authors M. Sakar gratefully acknowledges the NCNSNT-MHRD grants for the post-doctoral research fellowship, to carry out this research project. The authors VTPV and MC acknowledge the funding granted by the Ministry of Education, Youth and Sports in the framework of targeted support of 'National Programme for Sustainability I', OPR&DI project (LO1201) and OP VaVpI of the Centre for Nanomaterials, Advanced Technologies and Innovation CZ.1.05/2.1.00/01.0005.

Notes and references

1 Y. DU, M. LEI and H. YANG, *J. Mater. Sci. Technol*, 2008, **24**, 737.
2 L. E. Toth, Transition Metal Carbides and Nitrides Academic, New York, 1971.
3 H. Nakajima, Y. Ohashi and K. Shiiki, *J. Magn. Magn. Mater,* 1997, **167**, 259.
4 A. Sakuma, *J. Magn. Magn. Mater.*, 1991, **102**, 127.
5 S. Yamashita, Y.Masubuch, Y.Nakazawa, T.Okayama, M.Tsuchiya and S.Kikkawa, *J. Solid State Chem.,* 2012, **194**, 76.
6 D. M. Borsa and D. O. Boerma, *Hypetfine Interaction,* 2003, **151/152**, 31.
7 I. Nakatani and T. Furubayashi, *J. Magn. Magn. Mater.,* 1990, **85**, 11.
8 Y. Ohtsuka, C. Xu, D. Kong and N. Tsubouchi, *Fuel*, 2004, **83**, 685.
9 M. V. C. Sastri, R. P. Viswanath and B. Viswanathan, *Int. J. Hydrogen Energy,* 1982, **7**, 951.
10 N. S. Gajbhiy, R. N. Panda, R. S. Ningthoujam and S. Bhattacharyya, *phys. stat. sol. (c)*, 2004, **12**, 3252.
11 H. N. Fang, R. Zhang, B. Liu, Z. K. Tao, M. W. Xiao, X. F. Wang, Z. L. Xie, X. Q. Xiu and Y. D. Zheng, *AIP Advances,* 2013, **3**, 072136.
12 S. F. Matar, A. Houari, M. A. Belkhir and M. Zakhour, *Z. Naturforsch*, 2007, **62b**, 881.
13 R.S. Ningthoujam and N.S. Gajbhiye, *Mate. Res. Bul.,* 2008, **43**, 1079.
14 X. L. Wu, W. Zhong, N. J. Tang, H. Y. Jiang, W. Liu and Y. W. Du, *J. Alloys Comp.*, 2004, **385**, 294.
15 M. P. F. Garcıa, P. Gorria, M. Sevilla, A. B. Fuertes, R. Boada, J. Chaboy, G. Aquilanti and J. A. Blanco, *Phys. Chem. Chem. Phys.*, 2011, **13**, 927.
16 X. X. Zhang, G. H Wen, S. Huang, L. Dai, R. Gao and Z. L. Wang, *J. Magn. Magn. Mater.*, 2001, **231**, L9.
17 A. Demortiere, P. Panissod, B. P. Pichon, G. Pourroy, D. Guillon, B. Donnio and S. B. Colin, *Nanoscale*, 2011, **3**, 225.
18 Y. D. Zhang, J. I. Budnick and W. A. Hines, *Appl. Phys. Lett.*, 1998, **72**, 2053.
19 R. K. Zheng, G. H. Wen, K. K. Fung and X. X. Zhang, *Physical Review B*, 2004, **69**, 214431.
20 R. Prozorov, Y. Yeshurun, T. Prozorov and A. Gedanken, *Physical Review B*, 1999, **59**, 6956.